Downlink Massive MIMO Systems: Achievable Sum Rates and Energy Efficiency Perspective for Future 5G Systems

Joseph Isabona[1] · Viranjay M. Srivastava[1]

Abstract To meet up with the ever increasing subscribers' demand for higher data rates and mobile data traffic growth in the telecommunication industry, the fifth generation (5G) systems is being considered for the next future cellular communication standards. The two principal design requirements being aimed at in 5G are robust data transmission rates in Gigabits and low power consumption systems. Massive multiple input multiple output (M-MIMO) technology is an evolving smart antenna technology which has some key promising potentials to boost 5G networks in meeting the aforementioned requirements. However, there is an emergent concern that increased number of antenna arrays in M-MIMO system could induce high power consumption and poor energy efficiency when deployed at the base stations (BSs). Also, inter-cellular interference which occurs as a result of pilot contamination, fast fading and uncorrelated noise effects in the radio channels are other open issues in M-MIMO system. This work investigates and compare the achievable sum rates and energy efficiency of a downlink single cell M-MIMO systems utilizing linear and nonlinear precoding schemes. First, we have shown how the increasing signal-to-noise ratio and M-antennas impact the achievable sum rates. Furthermore, the energy saving potentials of M-MIMO systems in macro, micro and pico cellular environments when linear and nonlinear precoding schemes are utilized at the BS have been demonstrated. Particularly, by means of power fairness index, the tradeoff among the energy efficiency, sum rate and the system users have also been presented and discussed. Results show that substantial energy efficiency improvements can be achieved in micro and pico cellular environments of downlink M-MIMO systems when non-linear successive interference cancellation precoding is applied compared to linear precoding schemes.

✉ Joseph Isabona
josabone@yahoo.com

Viranjay M. Srivastava
viranjay@ieee.org

[1] Department of Electronic Engineering, Howard College, University of KwaZulu-Natal, Durban 4041, South Africa

1 Introduction

Since the early twentieth century, the breadth of wireless mobile communications has increased drastically (following what is as popularly known as Cooper's law). Till date, mobile subscribers are continuously embracing all sorts of contemporary wireless applications, such as real-time video streaming, machine-to-machine (M2M) communications, online movies, online gaming, mobile television, social networking, etc. According to Ericson mobility report in [1], the demand for higher data rates by subscribers and mobile data traffic grows about 60% on yearly basis. Thus, the next generation of mobile broadband systems, termed the fifth generation (5G) wireless communication systems, should be designed to meet up with this ever rapidly increasing demand for higher data rates.

One of the foremost or promising techniques to boost the future 5G systems in handing large subscriber density with higher data rate demands is multiuser antenna technology, known as M-MIMO. The M-MIMO is a smart antenna technology, where the base stations (BSs) are equipped with tens or hundreds of active antenna mechanisms. Presently, the MIMO technology has been incorporated into HSPA+ and LTE broadband cellular systems, based on 3GPP standard [2, 3] and other wireless standards such as WiMAX, 802.11n (WiFi) and 802.11ac (WiFi), though with different limitations. For example, the initial releases of 3GPP standard for LTE-advanced support up to 8 antennas at the base (BS) in a sectored topology and 4 antennas at the receiving user equipment (UE) terminals respectively [3].

Currently, for 5G cellular systems, M-MIMO is being considered as a potential enabling technology for its future realization. As a smart antenna technology, some of its promising benefits include: capability to accommodate large user traffic with high data rates quality, reduced latency, channel hardening, simplified media access control application, etc. However, the large number of transmit antennas in M-MIMO systems could also implies increase in power radiation and large amount of energy being consumed for signal processing at both the BSs and UE ends. This is because, as the number of antennas increases, there is also an upturn in the number of RF chains as well as the processing load. Another challenge is that the hardware (RF amplifier frontends) complexity of M-MIMO which grows exponentially as the transmitting antenna numbers increases [4]. Therefore, the radiated power need to be place under control in order to enhance system output efficiency [5]. Also, the inter-cellular interference which occurs as a result of pilot contamination [6], as well as the multifaceted architectural and heterogeneous takeoff plan of 5G systems could pose some challenges, especially in the area of precoding and detection algorithms.

The above highlighted challenges have been the prime focus of a number of research areas these days. Some of the different approaches that has been adopted by researchers in literature to look into the various challenges includes: effective multiuser antenna array design [7, 8], channel capacity analysis [9–12], practical MIMO channel measurement, modeling and analysis [13–18], transmitter precoding analysis [7, 19–25] and energy analysis [26–30].

Our area of interest in this work focus on transmitter precoding impact analysis with respect to achievable sum rates and energy consumption in M-MIMO systems.

Most of the previous research works on linear precoding focused on linear precoding analysis in multiuser MIMO systems, e.g. [26, 30]. For instance, in [26], performance investigation of M-MIMO system using linear ZF precoding algorithm in the downlink is presented. The authors showed that the deployment of M-MIMO system can improve its spectrum efficiency, outage probability and bit error rate. Similar performance investigation and analysis are also presented in [11, 27, 31, 32], but using other different linear detection or precoding schemes such as Matched filter (MF), Maximum ratio transmission (MRT), and minimum mean square error (MMSE).

In this work, the impact of both linear and non-precoding schemes such as MF, MMSE, ZF, and Successive Interference Cancellation (SIC) on M-MIMO systems is investigated in the downlink scenario. The primary motivation is to quantify the effect of multiuser interference suppressing capabilities of the various precoding schemes on sum rate capacity and energy efficiency of M-MIMO for generation wireless network systems such as 5G. Furthermore, the power saving potentials of very M-MIMO systems in macro, micro and pico cellular environments is also investigated. Particularly, we concentrate on how different precoding schemes and numbers of antennas impact the energy efficiency the M-MIMO systems. The trade-off between sum rate capacity and power resource distribution in M-MIMO systems is also examined.

The remaining part of this work is arranged into three sections. Section 2 presents the adopted single-cell M-MIMO model. A description of the considered linear and non-precoding schemes, along with power consumption models and energy efficiency metrics are also presented in Sect. 2. Results and analysis are provided in Sect. 3. Finally, Sect. 4 presents the conclusion of the work.

2 System Model

2.1 Channel Model

As presented in Fig. 1, we considered a downlink (i.e., forward link) single-cell M-MIMO model where a BS is equipped with M-antennas to serve K users ($M \geq K$), through
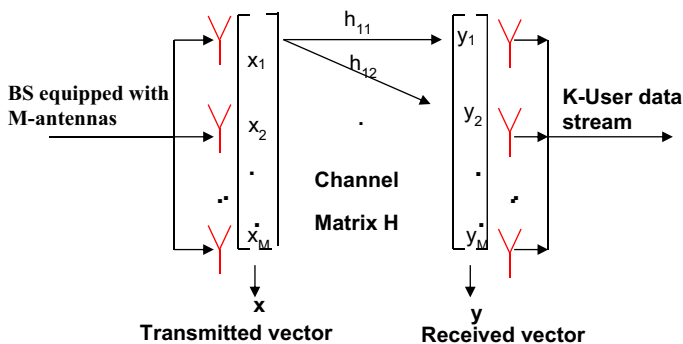

Fig. 1 Downlink M-MIMO system model with M-antennas and K-users

Rayleigh fading channels. With the assumption that the BS has perfect channel state information (CSI), the signal received vector at the K user terminals can be expressed as:

$$\mathbf{y}_{dl} = \sqrt{\rho_d}\mathbf{H}^T\mathbf{x} + \mathbf{n_d} \tag{1}$$

where $\mathbf{y}_{dl} \in C^{M \times 1}$ is the received signal vector at the kth user ($k = 1, 2, …, K$), $\mathbf{X} \in C^{M \times 1}$ is the signal vector transmitted at the base station such that $E\{\|\mathbf{x}\|\} = 1$, $\mathbf{n_d} \ CN(0, \sigma^2\mathbf{I})$ is the noise vector with $\mathbf{I}$, being the identity matrix. The superscript ''T'' symbolizes the transpose and ρ_d is the average SNR.

Also, assuming that the BS performs power allocation such that the SNR factor is equal for all K users to maximize their transmission rate, the sum-rate of kth user in the downlink can be expressed from the signal model of Eq. (2) as in [33]:

$$R_K = \max_{P_K} \log_2 \det\left(1 + \rho_d\mathbf{H}^T\mathbf{d_q}\mathbf{H}\right) \tag{2}$$

where $\mathbf{d_q}$ is the diagonal matrix with P_k diagonal elements for the kth users.

Then, downlink achievable sum-rate for the K user in the massive MIMO broadcast channel is well-defined by the maximum capacity of the entire users' data rates, R, in Eq. (3):

$$R = \sum_{k=1}^{M} R_k = 1 \tag{3}$$

2.2 Precoding Schemes

For optimum implementation of M-MIMO technology, the choice of precoding scheme plays a key role. Precoding is a method through which transmit diversity is exploited at the transmitter to send multiple data streams to the receiver with independent and appropriate weighting information streams. The fundamental task of the detector at the receiver is to reduce the effect of the received noise and interference, as well as to remove various forms of distortions due to the channel. Thus, precoding and detection are fundamental techniques of separating data streams and minimize inter-user interference at the BS and receiver user equipment.

There are basically two techniques of precoding: linear types, e.g. ZF, MMSE, MF and non-linear precoding, e.g. SIC, ML, etc.

2.2.1 Downlink Linear Precoding

Linear precoding is a transmitter-based precoding scheme for compensating for the multipath interfering effect of the communication channel. By means of linear precoding techniques in the downlink, the BS transmits linearly precoded information data with signal vector $\mathbf{x}$, which is predicated for the K users by:

$$\mathbf{x} = \sqrt{\alpha}\mathbf{W}\mathbf{q} \tag{4}$$

where $\mathbf{W} \in C^{M \times K}$ designates the precoding matrix, $\mathbf{q} \triangleq [q_1, q_2, …, q_k]^T$ denotes the signal vector which encloses the data symbols for the K user, and α represents the normalization constant which has been chosen subject to power constraint $E\{\|\mathbf{x}\|\} = 1$. Thus,

$$\alpha = \frac{1}{E\{tr(\mathbf{W}\mathbf{W}^T)\}} \tag{5}$$

Inserting (5) into (1), gives,

$$\mathbf{y}_{dl} = \sqrt{\alpha \rho_d}\,\mathbf{H}^T \mathbf{W}\mathbf{q} + n_d \tag{6}$$

$$\mathbf{y}_{dl} = \sqrt{\alpha \rho_d}\mathbf{H}_k^T \mathbf{w}_k q_k + \sqrt{\alpha \rho_d} \sum_{k^i \neq k}^{K} \mathbf{H}_k^T \mathbf{w}_{k^i} q_{k^i} + n_d \tag{7}$$

Therefore, the signal-to-interference-and-noise ratio (SINR) intended for the kth user from the BS is given by:

$$SINR_k = \frac{\alpha \rho_d \left|\mathbf{H}_k^T \mathbf{W}_k\right|^2}{\alpha \rho_d \sum_{k^i \neq k} \left|\mathbf{H}_k^T \mathbf{W}_k\right|^2 + \sigma^2} \tag{8}$$

2.2.2 Linear ZF Precoding

The ZF precoding is a well-known MIMO precoding method in literature. This is probably due to its low complexity nature and ZF precoding can be implemented without having any prior knowledge of noise statistics. The ZF precoding is basically employed at the BS to remove the inter-user interference when transmitting signals in the direction of the proposed user. Mathematically, the ZF precoder can be expressed as [34]:

$$\mathbf{W}_{ZF} = \left(\mathbf{H}^* \mathbf{H}^T\right)^{-1} \mathbf{H}^T \tag{9}$$

Thus, using $\mathbf{W}_{ZF}$, the transformed linear ZF precoding symbol estimate can be written as:

$$\hat{s} = Q[W_{ZF}y] = s + \left(\mathbf{H}^* \mathbf{H}^T\right)^{-1} \mathbf{H}^T v \tag{10}$$

$$Q[W_{ZF}y] = s + \left(\mathbf{H}^* \mathbf{H}^T\right)^{-1} \mathbf{H}^T v = s + \hat{v}_{ZF} \tag{11}$$

where $Q[\cdot]$ denotes the quantization operation and it maps the soft values toward nearest constellation point. s is the estimate of the transmitted symbol.

2.2.3 Linear MF Precoding

The MF is also one of the simplest and oldest precoding techniques in literature. It is often called the conventional filter or the maximum ratio transmission (MRT) [35, 36]. The MF precoding technique is applied to maximize the received SNR at the user mobile terminal. It can be determined by finding solution to the optimisation problem [36]:

$$M_{MF} = \arg \max_w \frac{E\{|s^T y|\}^2}{\sigma_n^2} \tag{12}$$

The solution to optimisation problem can expressed by:

$$W_{MF} = H^T \tag{13}$$

Thus, the MF precoding symbol estimate can be written as:

$$W_{MF}y = Q[H^T y] \tag{14}$$

2.2.4 Linear MMSE Precoding

The MMSE precoding can be generated by regularizing the pseudo-inverse of the channel matrix [34]:

$$\mathbf{W}_{MMSE} = (\alpha \mathbf{I} + \mathbf{H}^* \mathbf{H}^T)^{-1} \mathbf{H}^T \tag{15}$$

where α is a regularization factor.

The resultant output from the transmit antenna can be evaluated from:

$$\hat{s} = Q[\mathbf{W}_{MMSE}y] = (\alpha \mathbf{I} + \mathbf{H}^* \mathbf{H}^T)^{-1} \mathbf{H}^T y \tag{16}$$

$$= Q[\mathbf{W}_{MMSE}y] = \hat{s} + (\alpha \mathbf{I} + \mathbf{H}^* \mathbf{H}^T)^{-1} \mathbf{H}^T v = \hat{s} + \hat{v}_{MMSE} \tag{17}$$

2.2.5 Non-linear SIC Precoding

Non-linear precoding embroils additional signal processing technique compared to the linear precoding to deliver higher performance gains at the receiver. SIC is a suboptimal non-linear precoding technique which uses successive interference elimination method to improve information transmission at the BS, compared to linear ZF, MF and MMSE precoding. Thus, SIC precoding is specifically applied to cancel interference among antenna transmit streams of multiple data [37]. The SIC precoding can be obtain from the received signal vector in Eq. (1) as:

$$\mathbf{y}_i = \mathbf{y} - \sum_{j=1}^{i-1} \mathbf{h}_j s_j \tag{18}$$

where $\mathbf{y}_i$ and $\mathbf{h}_j$ indicate the signal received after the $k-1$th interference cancellation and the *j*th column vector of $\mathbf{H}$ respectively. S_j is the transmitted symbol.

An effective approach for SIC precoding can be realized either by using QR channel matrix decomposition (ZF approach [38, 39]) or the extended channel matrix (i.e., the MMSE approach) [40]. Here, our focus is on the MMSE approach.

Thus, with the knowledge of the channel matrix $\mathbf{H}$ in Eq. (15), we can express the filter matrix w_i for SIC as:

$$\mathbf{w}_i = (\alpha \mathbf{I} + \mathbf{H}_{i-1} \mathbf{H}_{i-1}^T)^{-1} \mathbf{h}_i \tag{19}$$

where the quantity H_{i-1} represents the column matrix of the channel matrix H.

Therefore, using the transformation matrix w_i, the resultant SIC solution is given by:

$$\hat{s}_i = Q[\hat{z}i] = Q[\mathbf{W}_i y_i] \tag{20}$$

where $\mathbf{H}_i$, and $\mathbf{y}_i$ are updated each time the symbol s_j is successfully transmitted.

The superiority of SIC precoding over the linear counterparts is in two aspects:

(i)   Interference nulling: data stream interferences that are yet to be detected are projected out

(ii) Interference cancelling: data stream interferences at the receiver is subtracted out.

Thus, the mathematical description of SIC precoding algorithm is presented as follows:

1. Input: $\mathbf{y}$, $\mathbf{H}$, M
2. Initialize: $\mathbf{y} = \mathbf{y_i}$, i $\leftarrow$ 1
3. Compute the filter weight matrix using (19):

$$\mathbf{w}_1 = \left(\alpha\mathbf{I} + \mathbf{H}_{i-1}\mathbf{H}_{i-1}^T\right)^{-1}\mathbf{h}$$

4. Obtain the dominant user k_i SINR with minimum MSE:

$$k1 = \arg\min_j\left(SINR_j\right)$$

5. Compute and apply the MMSE interference nulling:

$$\hat{z}_i = \mathbf{w}_i\mathbf{y}_i$$

6. Detect the estimates of k_i using (20):

$$\hat{s}_i = \mathrm{Q}\left[\hat{z}i\right]$$

7. Update the detected component after performing interference cancellation:

$$\mathbf{y}_{i+1} = \mathbf{y}_i - \mathbf{y}_{i-1}\hat{s}_i$$

8. Update $\mathbf{H}_i = [\mathbf{h}_{i+1}\mathbf{h}_{i+2}\cdots\mathbf{h}_M]$
9. *end*

The achieved output SIC *SINR* of the *k*th user, is given by [41]:

$$SINR_{SIC,k} = \gamma_{SIC,k} = \mathbf{h}_k^H\left(\sum_{l=k+1}^{M}\left(\frac{P}{K\sigma^2}\mathbf{I} + \mathbf{h}_l\mathbf{h}_l^T\right)^{-1}\right)\mathbf{h}_K \tag{21}$$

The SINR for the MMSE can be determined from SIC by replacing $\sum_{l=k+1}^{M}\mathbf{h}_k\mathbf{h}_k^T$ with $\sum_{l=1,l\neq k}^{M}\mathbf{h}_l\mathbf{h}_l^T$ in Eq. (21) and this result to the expression in Eq. (22):

$$SINR_{MMSE,k} = \gamma_{MMSE,k} = \mathbf{h}_k^H\left(\sum_{l=1,l\neq k}^{M}\left(\frac{P}{K\sigma^2}\mathbf{I} + \mathbf{h}_l\mathbf{h}_l^T\right)^{-1}\mathbf{h}_K\right) \tag{22}$$

Looking closely at Eqs. (21) and (22), it is obvious that $\sum_{l=k+1}^{M}\mathbf{h}_l\mathbf{h}_l^T \geq \sum_{l=1,l\neq k}^{M}\mathbf{h}_l\mathbf{h}_l^T$, thus maximizing the information signal can be conveyed with $SINR_{SIC}$ than with $SINR_{MMSE}$. This validates the superiority of SIC precoding over MMSE precoding. The equality between the two output SINR only hold on the condition that $\sum_{l=1}^{M}\mathbf{h}_l\mathbf{h}_l^T = 0$.

Therefore, achievable rate, R of the user data stream with SIC can be determined from the $SINR_{SIC}$ model by:

$$R_{SIC,k} = \log_2\left[1 + \frac{P}{K\sigma^2}\mathbf{h}_k^H\left(\mathbf{I} + \sum_{l=k+1}^{M}\frac{P}{K\sigma^2}\mathbf{h}_l\mathbf{h}_l^T\right)^{-1}\mathbf{h}_k\right] \tag{23}$$

$$R_{SIC,k} = \log_2 \det \left[\mathbf{I} + \left(\frac{P}{K\sigma^2} \sum_{l=k+1}^{M} \mathbf{h}_l \mathbf{h}_l^T + \mathbf{I} \right)^{-1} \frac{P}{K\sigma^2} \mathbf{h}_k^H \mathbf{h}_K \right] \tag{24}$$

$$R_{SIC,k} = \log_2 \det \left[\mathbf{I} + \frac{P}{K\sigma^2} \left(\mathbf{I} + \sum_{l=k+1}^{M} \frac{P}{K\sigma^2} \mathbf{h}_l \mathbf{h}_l^T \right)^{-1} \mathbf{h}_k \mathbf{h}_k^T \right] \tag{25}$$

Similar to Eq. (1), the expression in Eq. (25) can be simplified further using the principle of identity matrix inversion to yield:

$$R_{SIC,k} = \log_2 \det \left(\mathbf{I}_M + \frac{P}{K\sigma^2} \mathbf{H}\mathbf{H}^T \right) \tag{26}$$

Accordingly, the achievable sum rate of the K users is defined by:

$$R_{sum} = \sum_{k=1}^{K} \mathrm{E} \left[\log_2 \left(1 + SINR_{SIC,k} \right) \right] \tag{27}$$

where $\mathrm{E}[\cdot]$ designates statistical expectation.

2.3 Energy Efficiency and Power Consumption Model

2.3.1 Power Consumption Model

In recent time, energy efficiency (EE) assessment has received considerable attention in wireless communication systems. This is as a result of increasing interest in green communications and their energy consumption optimisation. In this section, to examine the tradeoff between the energy consumption and the achieved sum rates in M-MIMO systems under the different precoding schemes, we consider a linearised BS power (P_{BS}) that has been widely used in literature for energy efficiency evaluation. It is given as [42–44]:

$$P_{BS} = \frac{1}{\eta} P_t + M P_C + P_0 \tag{28}$$

where η and P_o account for power amplifier efficiency and non-transmission power consumption respectively. P_c denotes circuit power efficiency due to RF chain and P_t denotes the BS transmits power as shown in Table 1.

2.3.2 Energy Efficiency Metrics

The following energy efficiency metrics are considered in this research work.

Table 1 BS Power consumption parameters for cell type [42, 45]

BS cell type	η	P_t (W)	P_c (W)	P_o (W)
Macro	0.14	80	244	225
Micro	0.32	6.3	35	34
Pico	0.23	0.25	6.1	2.6

(a)   The energy throughput ratio (ETR): is an important performance metric for assessing system energy efficiency. It is determined by the expression [45]:

$$ETR = \frac{P_{BS}}{T_p^2} \tag{29}$$

where T_P is the throughput and it is defined as the mean of the sum rate over all the feasible users' rate R_k (in bit/s/Hz). P_{BS} represents power consumption due to BS.

(b)   The Power Fairness Index (PFI) is another performance metric and it reflects how the system resources are distributed among the users. Here, the Jain's power fairness index is considered and it is given by [46]:

$$PFI = \frac{\left(\sum\limits_{k=1}^{K} (P_{BS})_K / R_K\right)}{\sum\limits_{k=1}^{K} (P_k / R_K)^2} \tag{30}$$

3 Simulation Results and Analysis

In order to validate the theoretical analysis presented previously, we conducted a system level simulation using a MATLAB 2013a. The power consumption model parameters used for simulation are shown in Table 1. The performance metric considered for analysis includes the sum rate capacity, energy throughput ratio and power fairness index.

To begin with, the simulation results of M-MIMO and conventional MIMO performance, in terms of sum rate capacity versus increasing SNR, is illustrated in Fig. 2. As in Fig. 2, the achievable sum rate of massive MIMO system outperformed that of the conventional MIMO for any value of SNR. The performance gain of M-MIMO can be attributed to its enhanced spatial multiplexing and antenna array gain which maximizes transmission rates as well as its ability to exploit higher degree of multiuser diversity (large diversity gain) as the number of antennas grows at users.

Fig. 2 Sum rate capacity comparison between M-MIMO and conventional MIMO Systems
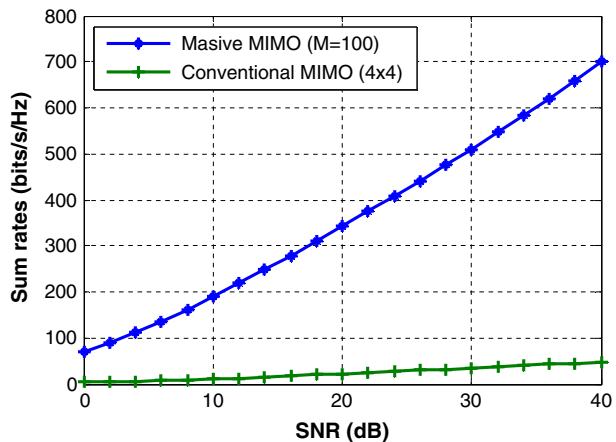
Figures 3, 4 and 5 display the achieved sum rate with MMSE, SIC and ZF precoding for M = 20, 50 and 80 respectively. For all values of M as shown in the figures, it is plainly seen that SIC consistently outperforms MF, MMSE and ZF over the whole span of SNR. For example, with M = 80 as provided in Fig. 4, SIC performance improvement over MMSE and ZF is about 4 and 5 dB, away from the ZF. The improvement accomplished by SIC stem from its post interference detection, suppression and cancellation capabilities. Also, it is interesting to observe in Fig. 4 that MMSE and ZF tend to perform seemingly at high values of SNR. But as M increases, the advantage of MMSE over ZF begins to grow quickly as noticeably seen in Figs. 3 and 4. Also, in the low region of the graphs, it is clearly seen that the MF filter achieved higher sum rates than the ZF; thus in this region, interference would better be treated as noise. Conversely, the poor interference suppression limitation nature of MF is clearly seen in Figs. 2, 3 and 4, as its achievable sum rates saturate with increasing SNR especially at values, as compared to ZF, MMSE and SIC that have steady performance improvement. Similar results for MF have also been reported in [34].

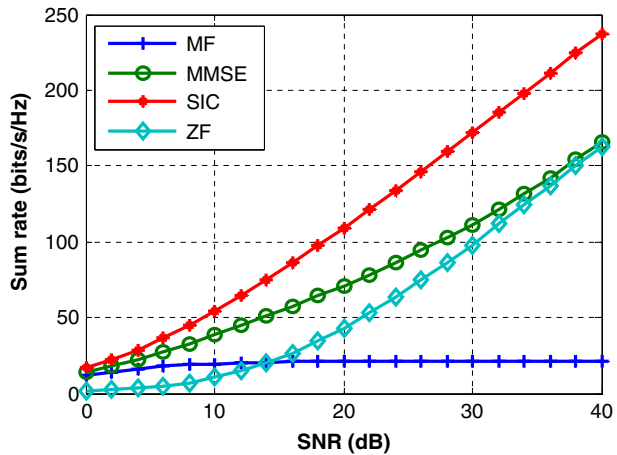Fig. 3 Achievable sum rate versus increasing SNR values with M = 20

Fig. 4 Achievable sum rate versus increasing SNR values with M = 50
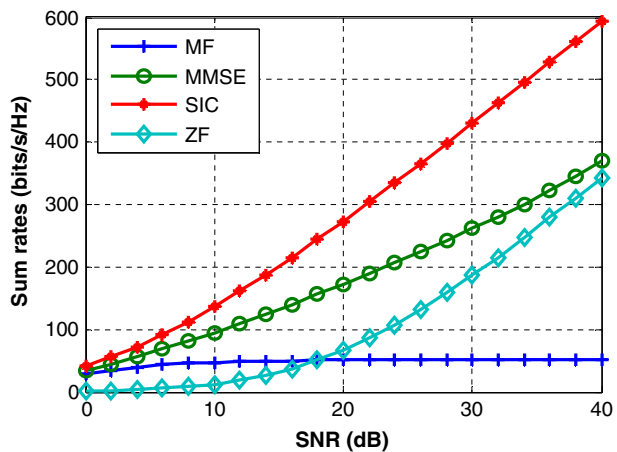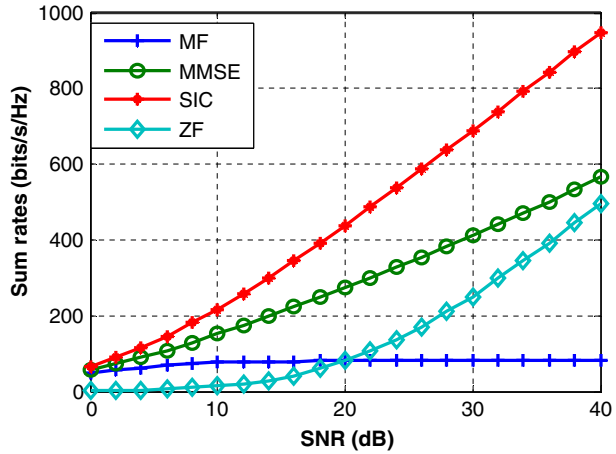
Fig. 5 Achievable sum rate versus increasing SNR values with M = 80

In Figs. 6, 7 and 8, the sum rate versus M-antennas are plotted by keeping SNR constant at 16, 26 and 30 dB respectively during simulation. It is notice that that the sum rate increase with M due to intensification of degrees or dimension of freedom. Again, the performance gain of the non-linear SIC precoding scheme over others is clearly seen due to its superior interference suppression and cancellation abilities.

Figures 9, 10 and 11 depict the ETR performance by comparing the non-linear SIC precoding scheme with other linear ones at M = 80 and SNR = 10 in macrocell, microcell and picocell environment. A lower ETR indicates a better energy-efficient system. From the simulation results of Figs. 8, 9 and 10, it is observed that the ETR decreases with increase in the number of users. Again, the superior interference suppression capacity of SIC algorithm over others has enable it to produce a more stable and better ETR values, except in the macrocell. Moreover, by quantitatively looking at Figs. 9, 10 and 11, it is observed that the picocell recorded about 20 and 30% ETR performance gains (i.e., more energy efficiency) compared to microcells and macrocells. This can be as a results of small

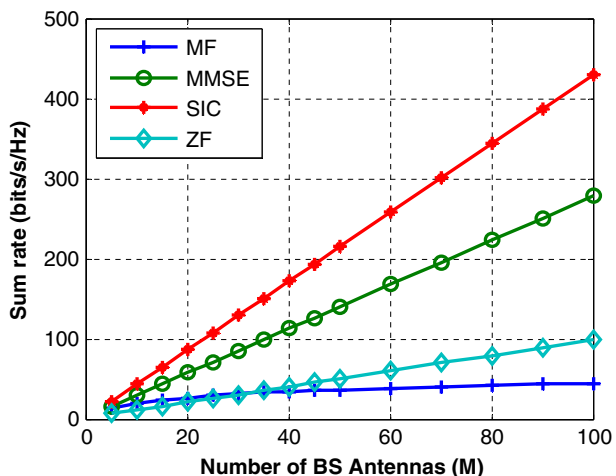**Fig. 6** Achievable sum rate versus M-antennas with SNR = 16 dB

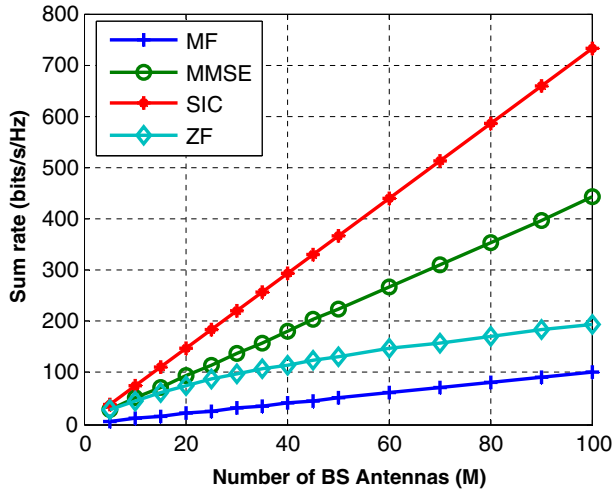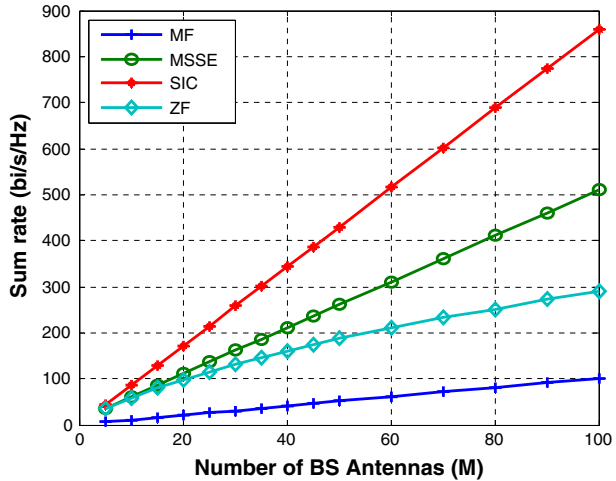Fig. 7 Achievable sum rate versus M-antennas with SNR = 26 dB

Fig. 8 Achievable sum rate versus M-antennas with SNR = 30 dB

cell structure of picocells and their ability to balance consumption power in correspondence with the current activity level.

Fairness index indicates how equitable the system resources are allotted to the users. Figure 12 shows that the MF precoding attains the highest fairness with increasing number of users, K. This occurs due to throughput-fairness index tradeoffs. This also implies that achieving fairness during resource allocation among users comes at the cost of system throughput reduction.

Furthermore, Fig. 13 is plotted to examine how fairly the power resources is allocated to users in M-MIMO systems with different precoding schemes using survival function plot. The survival function plot is one of the strategic ways of displaying and describing survival data in engineering. It is related to cumulative distribution function (CDF) by $S(t) = 1 - CDF$, where $S(t)$ is the function. For example, taking 0.3 as a fairness index reference point (horizontal axis) with survival function (vertical axis) in Fig. 12, it is

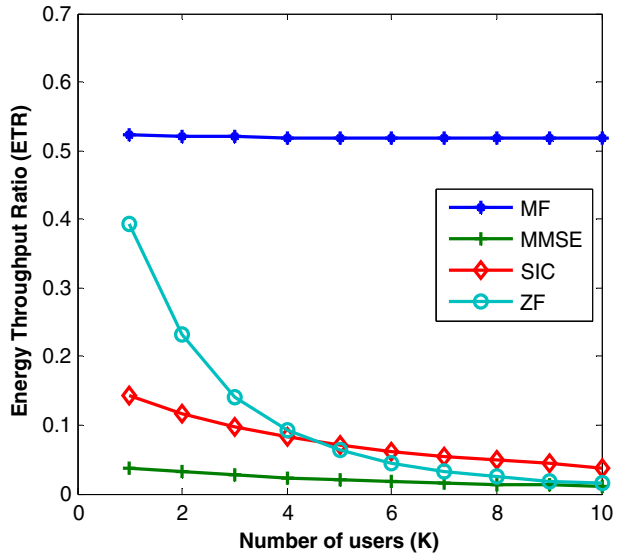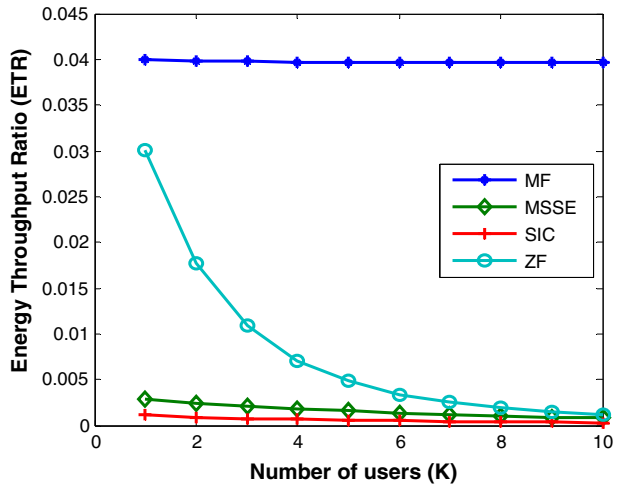**Fig. 9** Macrocell energy throughput ratio with M = 80

Fig. 10 Microcell energy throughput ratio with M = 80

observed that ZF, SIC, MMSE and MF have 0.15, 0.62, 0.63 and 0.91 survival respectively. Again, the results indicate throughput-fairness index tradeoffs.

Using ZF and MMSE as case in point, the graphs in Figs. 14 and 15 are plotted to examine the impact of increasing M-antennas on power resource fairness distribution among cell users. It is worth mentioning from the graphs that the fairness in distributing the system resources improves with increasing M. Specifically, a closer observation indicates that fairness index improves by about 20% when M increases by 2.5. This implies that less power is expended as consumption as the number of M antenna increases, thus leading to a more efficient energy system. It is expected that SIC and MF will have similar better-quality performance trend with increasing M antennas.

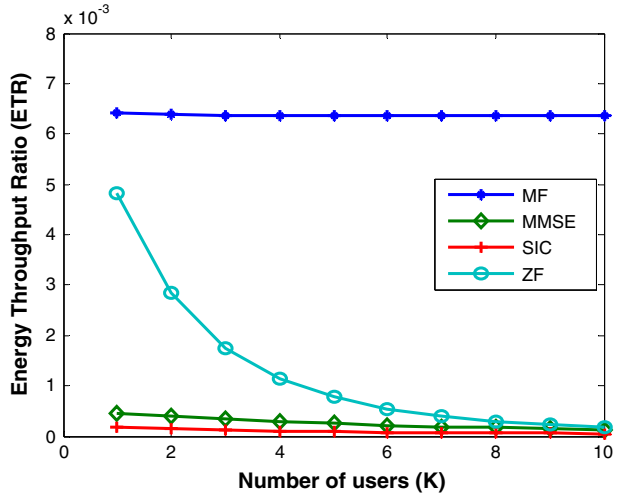**Fig. 11** Picocell energy throughput ratio with M = 80

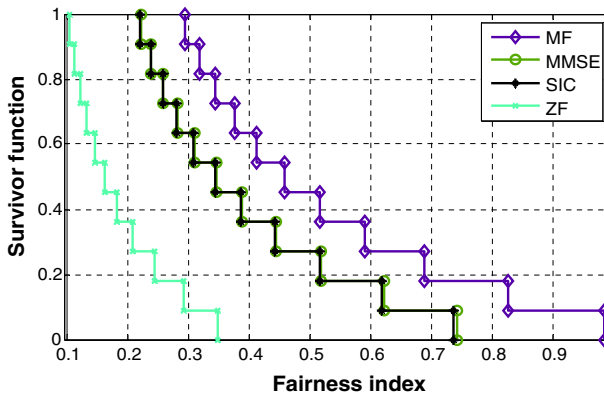**Fig. 12** Survival function versus system users for Macrocell
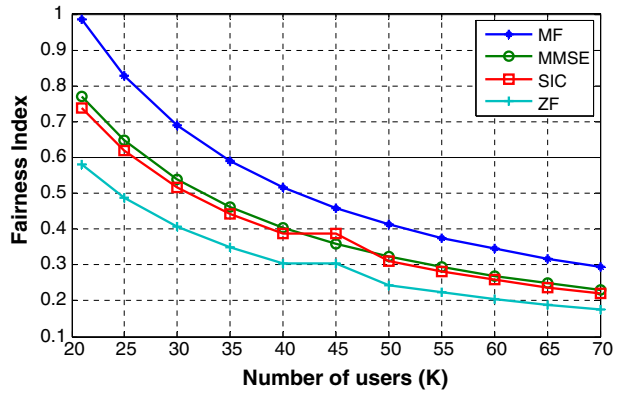

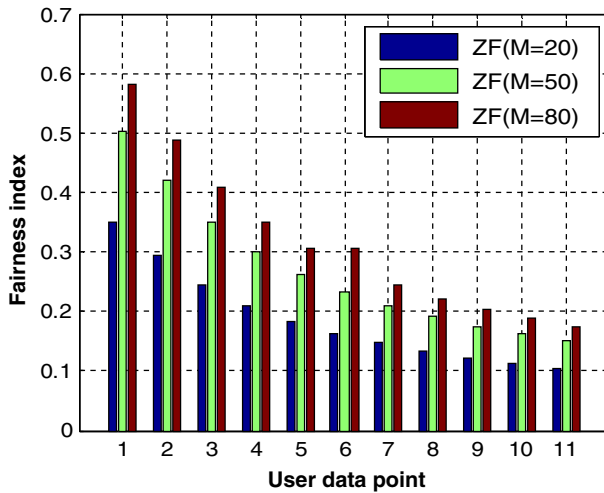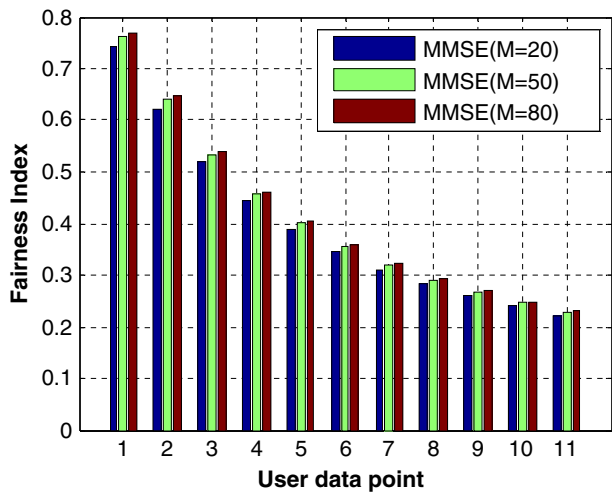**Fig. 13** Survival function versus fairness index for Macrocell

Fig. 14 Fairness index versus user data points with ZF precoding in macrocell

Fig. 15 Fairness index versus user data points with MMSE precoding in macrocell

4 Conclusion

In this work, the achievable sum rates and energy efficiency of a single cell M-MIMO systems utilizing linear and nonlinear precoding schemes have been investigated and compared in the downlink scenario. Specifically, the effects of signal-to-noise ratio (SNR) and increasing number of M-antennas on the mean user sum rates have been shown. We provided an insight on the power saving potentials of M-MIMO systems in macro, micro and pico cellular environments utilizing linear and nonlinear precoding schemes. Also, by using the power fairness index, the tradeoff among the energy efficiency, sum rate and the system users are presented and discussed. In summary, the simulation results indicate that a significant performance gain can be achieved in terms of energy efficiency when nonlinear

precoding schemes such as the successive interference cancellation (SIC) is applied in a downlink M-MIMO system technology as compared to the linear precoding schemes.

In future work, we will investigate the impact of the hardware impairments, hardware complexity due to increase in radio frequency chains, and pilot overhead issues in M-MIMO systems.

References

1. Ericson Mobility Report on the Pulse of the Network Society (2016). Revision A (pp. 1–32).
2. Dahlman, E., Parkvall, S., & Beming, P. (2008). *3G evolution HSPA and LTE for mobile broadband* (1st ed.). London: Academic Press.
3. Boccardi, F., Clerckx, B., Ghosh, A., Hardouin, E., Jongren, G., Kusume, K., et al. (2012). Multiple-antenna techniques in LTE-advanced. *IEEE Communications Magazine, 50*(3), 114–121.
4. Suthisopapany, P., Meesomboony, A., Kasaiz, K., & Virasit, I, (2012) Ultra low complexity soft output detector for non-binary LDPC coded large MIMO systems. In *International symposium on Turbo codes and iterative information processing (ISTC), Gothenburg* (pp. 230–234).
5. Hiaohu, G., Cheng, H., Guizani, M., & Han, T. (2014). 5G wireless backhaul networks: Challenges and research advances. *IEEE Network, 28*(6), 6–11.
6. Marzetta, T. L. (2010). Noncooperative cellular wireless with unlimited numbers of base station antennas. *IEEE Transaction on Wireless Communication., 9*(11), 3590–3600.
7. Alrabadi, O. N., Tsakalaki, E., Huang, H., & Pedersen, G. F. (2013). Beamforming via large and dense antenna arrays above a clutter. *IEEE Journal on Selected Areas in Communications, 31*(2), 314–325.
8. Taluja, P. S., & Hughes, B. L. (2013). Diversity limits of compact broadband multi-antenna Systems. *IEEE Journal on Selected Areas in Communications, 31*(2), 326–337.
9. Rusek, F., Persson, D., Lau, B. K., & Larssonet, E. G. (2012). Scaling up MIMO: Opportunities and challenges with very large arrays. *IEEE Signal Processing Magazine, 30*(1), 40–60.
10. Leeand, C., & Chae, C. B. (2012). Network massive MIMO for cell-boundary users: From a Precoding normalization perspective. In *International workshop on cloud base-station and large-scale cooperative communications* (pp. 233–237).
11. Hoydis, J., Brink, S. T., & Debbah, M. (2013). Massive MIMO in the UL/DL of cellular networks: How many antennas do we need? *IEEE Journal on Selected Areas in Communications, 31*(2), 160–171.
12. Yang, W., Durisi, G., & Riegler, E. (2013). On the capacity of large-MIMO block-fading channels. *IEEE Journal on Selected Areas in Communications, 31*(2), 117–132.
13. Hoydis, J., Hoek, C., Wild, T., & ten Brink, S. (2012). Channel measurements for large antenna arrays. In *International symposium on wireless communication systems (ISWCS), Paris* (pp. 811–815).
14. Marzetta, T. L. (2015). Massive MIMO: An introduction. *Bell Labs Technical Journal, 20*, 11–22.
15. Payami, S., & Tufvesson, F. (2012). Channel measurements and analysis for very large array systems at 2.6 GHz. In *6th European conference on antennas and propagation (EuCAP) 2012, Prague, Czech Republic* (pp. 1–5).
16. Gao, X., Tufvesson, F., Edfors, O., & Rusek, F. (2012). Measured propagation characteristics for very-large MIMO at 2.6 GHz. In *Conference on signals, systems and computers (ASILOMAR)* (pp. 295–299).
17. Gao, X., Tufvesson, F., & Edfors, O. (2013). Massive MIMO channels—Measurements and models. In *Asilomar conference on signals, systems and computers, Pacific Grove, CA* (pp. 280–284).
18. Martınez, A. O., De Carvalho, E., & Nielsen, J. O. (2014).Towards very large aperture massive MIMO: A measurement based study. In *IEEE Globecom workshops (GC Wkshps), Austin, TX* (pp. 281–286).
19. Gao, X., Edfors. O., & Rusek, F. (2011). Linear pre-coding performance in measured very-large MIMO channels. In *IEEE vehicular technology conference (VTC Fall)* (pp. 1–5).
20. Yang, H., & Marzetta, T. L. (2011). Performance of conjugate and zero-forcing beamforming in large-scale antenna systems. *IEEE Journal on Selected Areas in Communications, 31*(2), 172–179.
21. Guthy, C., Utschickand, W., & Honig, M. L. (2010). Large system analysis of the successive encoding successive allocation method for the MIMO BC. In *International ITG workshop on smart antennas (WSA)* (pp. 226–231).
22. Artigue, C., & Loubaton, P. (2011). On the precoder design of flat fading MIMO systems equipped with MMSE receivers. A large-system approach. *IEEE Transactions on Information Theory, 57*(7), 4138–4155.

23. Jose, J., Ashikhminand, A., & Marzetta, T. L. (2011). Pilot contamination and precoding in multi-cell TDD systems. *IEEE Transactions on Wireless Communications, 10*(8), 2640–2651.
24. Appaiah, K., Ashikhminand, A., & Marzetta, T. L. (2010). Pilot contamination reduction in multi-user TDD systems. *IEEE international conference on communications (ICC)*, pp.1–5.
25. Ashikhminand, A., & Marzetta, T. (2012). Pilot contamination precoding in multi-cell large scale antenna system. In *IEEE international symposium on information theory proceedings* (pp. 1137–1141).
26. Zhao, L., Zheng, K., Long, H., & Zhao, H. (2014). Performance analysis for downlink massive MIMO system with ZF precoding. *Transaction on Emerging Telecommunication Technology, 25,* 1219–1230.
27. Ngo, H. Q., Larsson, E. G., & Marzetta, T. L. (2013). Energy and spectral efficiency of very large multiuser MIMO systems. *IEEE Transactions on Communications, 62*(4), 1436–1449.
28. Huh, H., Caire, G., Papadopoulos, H. C., & Ramprashad, S. A. (2012). Achieving massive MIMO spectral efficiency with a not-so-large number of antennas. *IEEE Transactions on Wireless Communication, 11*(9), 3226–3239.
29. Xu, Y., Xia, X., Ma, W., Zhang, D., Xu, K., & Wang, Y. (2015), Full-duplex massive MIMO relaying: An energy efficiency perspective. *Wireless Personal Communications, 84*(3), 1933–1961. http://link.springer.com/journal/11277/84/3/page/1.
30. Li, L. (2013). Advanced channel estimation and detection techniques for MIMO and OFDM systems. Ph.D. thesis, University of York (pp. 1–194).
31. Rusek, F., Persson, D., & Lau, B. K. (2013). Scaling up MIMO: Opportunities and challenges with very large arrays. *IEEE Signal Processing Magazine, 30*(1), 40–60.
32. Yang, H., & Marzetta, T. L. (2013). Performance of conjugate and zero-forcing beamforming in large-scale antenna system. *IEEE Journal on Selected Areas in Communications, 31*(2), 172–179.
33. Ngo, H. Q. (2015). Massive MIMO: Fundamentals and system designs. Ph.D. thesis, Department of Electrical Engineering, Linkoping University.
34. Huang, H., Papadias, C. B., & Venkatesan, S. (2012). *MIMO communication for cellular networks*. New York, NY: Springer.
35. Verdu, S. (1998). *Multiuser detection*. Cambridge: Cambridge University Press.
36. Utschick, W., & Josef, A. (2005). Linear transmit processing in MIMO communications systems. *IEEE Transactions on Signal Processing, 53*(8), 2700–2712.
37. Sadek, M., Tarighat, A., & Sayed, A. H. (2007). Active antenna selection in multiuser MIMO communications. *IEEE Transactions on Signal Processing, 555*(4), 1498–1510.
38. Wubben, D., Bohnke, R., Kuhn, V., & Kammeyer, K. D. (2003). MMSE extension of V-BLAST based on sorted QR decomposition. In *Vehicular technology conference, VTC 2003-Fall* (pp. 508–512).
39. Mandloi, M., Hussain, M. A., & Bhatia, V. (2016). An improved multiple feedback successive interference cancellation algorithm for MIMO detection. In *International conference on communication systems and networks (COMSNETS), Bangalore* (pp. 1–6).
40. Kobayashi, R. T., Ciriaco, F., & Abrao, T. (2014). Performance and complexity analysis of suboptimum MIMO detectors under correlated channel. In *Telecommunications symposium (ITS), 2014 international, Sao Paulo* (pp. 1–5).
41. Tse, D., & Viswanath, P. (2004). Fundamental of wireless communications. Cambridge University Press. ISBN-10: 0521845270.
42. Auer, G., Blume, O., Giannini, Z., Godor, I., Imran, M. A., Jading, Y., et al. (2012). D2.3: Energy efficiency analysis of the reference systems, areas of improvements and target breakdown. In *INFSO-ICT-247733 energy aware radio and network technologies* (pp. 1–68).
43. Quek, T. Q. S., Cheung, W. C., & Kountouris, M. (2011). Energy efficiency analysis of two-tier heterogeneous networks. In *Proceedings of wireless conference on sustainable wireless technologies* (pp. 1–5).
44. Chang, L., Zhang, J., & Letaief, K. B. (2013). Energy efficiency analysis of small cell networks. In *IEEE ICC selected areas in communications symposium* (pp. 4404–4408).
45. Bohli, A., & Bouallegue, R. (2014). Energy efficiency in heterogeneous wireless networks using cognitive monitoring strategy. In *Modelling symposium (EMS), 2014 European, Pisa, 2014* (pp. 387–391).
46. Beh, K. C., Han, C., Nicolaou, M., Armour, S., & Doufexi, A. (2009). Power efficient MIMO techniques for 3GPP LTE and beyond. In *Vehicular technology conference fall (VTC 2009-Fall), Anchorage, AK* (pp. 1–5).

Joseph Isabona, Ph.D. is a Post-Doctoral Researcher in the Department of Electronic Engineering, Howard College, University of KwaZulu-Natal, Durban, South Africa. He received Ph.D. and M.Sc. degrees in Communication Electronics, 2013 and 2007 respectively, and a B.Sc. in Applied Physics in 2003. He has published both nationally and internationally in the area of Wireless Mobile Communications. His area of interest is RF Propagation Modelling and Radio Resource Management in Wireless Networks.

Prof. Viranjay M. Srivastava is Doctorate (2012) in the field of RF Microelectronics and VLSI Design from Jaypee University of Information Technology, Solan, Himachal Pradesh, India and received the Master degree (2008) in VLSI design from Centre for Development of Advanced Computing (C-DAC), Noida, India and the Bachelor degree (2002) in Electronics and Instrumentation Engineering from the Rohilkhand University, Bareilly, India. He was with the Semiconductor Process and Wafer Fabrication Centre of BEL Laboratories, Bangalore, India, where he worked on characterization of MOS devices, fabrication of devices and development of circuit design. Currently, he is a faculty in Department of Electronics Engineering, School of Engineering, Howard College, University of KwaZulu-Natal, Durban, South Africa. His research and teaching interests includes VLSI design, Nanotechnology, RF design and CAD with particular emphasis in low-power design, Chip designing, Antenna Designing, VLSI testing and verification and Wireless communication systems. He has more than 12 years of teaching and research experience in the area of VLSI design, RFIC design, and Analog IC design. He has supervised a number of B.Tech., M. Tech. and Ph.D. theses. He is a member of IEEE, IITPSA, ACEEE and IACSIT. He has worked as a reviewer for several conferences and Journals both national and international. He is author of more than 80 scientific contributions including articles in international refereed Journals and Conferences and also author of following books, (1) *VLSI Technology,* (2) *Characterization of C–V curves and Analysis, Using VEE Pro Software: After Fabrication of MOS Device*, and (3) *MOSFET Technologies for Double-Pole Four Throw Radio Frequency Switch*, Springer International Publishing, Switzerland, October 2013.